

Design of Multiple Trellis-Coded Multi-h CPM Based on Super Trellis

LIU Xian, LIU Aijun, ZHANG Bangning, PAN Kegang

Institute of Communications Engineering, PLA University of Science and Technology, Nanjing 210007, China

liuxianliuxian1981@163.com

Abstract. *It has been shown that the multiple trellis code can perform better than the conventional trellis code over AWGN channels, at the cost of additional computations per trellis branch. Multiple trellis coded multi-h CPM schemes have been shown in the literature to have attractive power-bandwidth performance at the expense of increased receiver complexity. In this method, the multi-h format is made to be associated with the specific pattern and repeated rather than cyclically changed in time for successive symbol intervals, resulting in a longer effective length of the error event with better performance. It is well known that the rate $(n-1)/n$ multiple trellis codes combined with 2^n -level CPM have good power-bandwidth performance. In this paper, a scheme combining rate $1/2$ and $2/3$ multiple trellis codes with 4- and 8-level multi-h CPM is shown to have better power-bandwidth performance over the upper bound than the scheme with single-h.*

Keywords

Multiple trellis code, multi-h continuous phase modulation, merged encoder, super trellis.

1. Introduction

With the adoption of MIL-STD-188-181B on 20 March 1999 [1], Multi-h Continuous Phase Modulation (CPM) became a mandatory requirement of US Military UHF SATCOM terminals. A dual-h CPM scheme (with two distinct modulation indices) was selected as a Tier-II waveform in IRIG-106 Aeronautical Telemetry (ARTM) standard in 2004 because of its superior spectral efficiency and error performance as compared to the legacy PCM/FM (Pulse Code Modulation/Frequency Modulation) waveforms [2].

In these multi-h CPM schemes, a properly chosen cyclic set of modulation indices results in delayed merging of neighboring phase trellis paths and therefore, provides a larger minimum Euclidean distance than conventional single-h CPM schemes. The error performance for multi-h CPM schemes on AWGN and flat fading channels were presented in [3] and [4] respectively. However, most multi-

h schemes change the modulation index in a cyclical fashion for successive symbol intervals. Bhumi A. Dave and Raveendra K. Rao described a class of CPM signals referred to as generalized asymmetric multi-h phase-coded modulation which adaptively changed modulation indices by a function of the current symbol, previous symbol and phase state and hence could achieve significant amount of increase in minimum distance as compared to ordinary multi-h CPM signaling [5].

Trellis coded multi-h CPM schemes using a Viterbi decoder has been investigated to achieve further coding gains [6], [7], in which trellis paths remained unmerged longer and offered generally improved minimum Euclidean free distance. This scheme results in a kind of concatenated code and provides better performance with properly chosen modulation indices [8–11]. A nonlinear CPM technique is presented in [12] which achieves the maximal constraint length allowed by the number of states and achieves attractive minimum distances compared with other existing CPM signaling formats. However, maximization of the constraint length does not ensure the maximization of the minimum distance and hence this technique does not guarantee the highest achievable minimum distance. This technique also has the disadvantage of using a large number of modulation indices.

The multiple trellis code, wherein more than one channel symbol per trellis branch is transmitted, could usually provide superior performance [13]. Such mechanism accommodates more freedom for the assignment of signal points to transmitted symbols, and thus for many cases, produce better codes. Although the multiple trellis code is a powerful code, the branch extension operations required for the transition between states are more complex than that in the conventional trellis code.

In this paper, we propose a design procedure based on super trellis of the merged encoder combined by multiple trellis encoder and CPE (Continuous Phase Encoder). System performance in AWGN channel is analyzed based on the minimum squared Euclidean free distance dominated by the minimal error event of the merged encoder.

The remainder of this paper is organized as follows. System model and the merged encoder constructed by multiple trellis encoder and CPE are given in Section 2.

Super trellis structure of the merged encoder is presented in Section 3. Section 4 presents the design procedure of the multiple trellis coded multi-h CPM system to achieve superior performance. Performance analysis is described in Section 5 and numerical results and discussion are given in Section 6. Finally, conclusions are drawn in Section 7.

2. System Model

2.1 Multiple Trellis Coded Multi-h CPM System Description

The multiple trellis coded multi-h CPM system considered in this paper is shown in Fig. 1. At epoch n , the source information bit b_n is input to a multiple trellis encoder whose output is code symbol U_n from the M -ary alphabet $\{0, 1, \dots, M-1\}$. The code symbol U_n is fed into CPE whose output $\chi_n^{(\gamma)}$ is input to memoryless modulator (MM) which completely specifies the physical phase and therefore, completely specifies the output signal. The two sub-encoders construct the merged encoder, and the analysis of overall error event is based on such merged encoder.

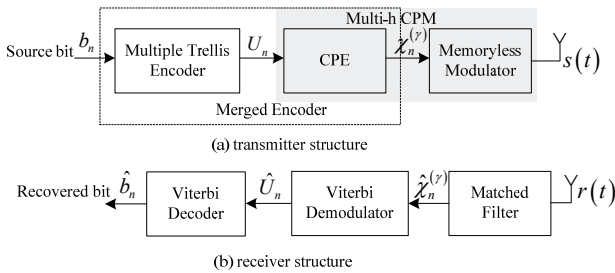


Fig. 1. Transmitter/Receiver structure of multiple trellis coded multi-h CPM system.

For AWGN channels, the received signal is

$$r(t) = s(t) + n(t) \quad (1)$$

where $n(t)$ is a Gaussian random process with power spectral density N_0 W/Hz. The received signal is fed into matched filter whose output $\hat{\chi}_n^{(\gamma)}$ is input to Viterbi demodulator. The output of demodulator \hat{U}_n is input to Viterbi decoder whose output \hat{b}_n is the recovered information bits.

2.2 Decomposition of Multi-h CPM

Rimoldi presented a tilted phase description of the single-h CPM signals in [14] by shifting the carrier frequency from f_0 to $f_1 = f_0 - \pi h(M-1)/2T$, where h is the modulation index, T is the symbol interval. The resulting modified phase (tilted phase) trellis is time invariant, and the single-h CPM modulator can be interpreted as a cascade of a linear CPE and a memoryless modulator. Saleem

and Stüber showed that the tilted phase representation of multi-h CPM signals results in a periodic phase trellis in [15], which enables the decomposition of multi-h CPM modulator as a cascade of a periodic recursive CPE and a memoryless modulator.

First, the complex envelope of a multi-h CPM waveform with H different modulation indices is given by

$$s(t, \mathbf{U}) = \sqrt{\frac{E}{T}} \exp\{j(\phi(t, \mathbf{U}) + \phi_0)\}, t \geq 0 \quad (2)$$

where E is the energy per symbol, ϕ_0 is a constant phase term which can be ignored if phase synchronization is assumed. The time varying phase $\phi(t, \mathbf{U})$, also called the excess phase, is defined as

$$\phi(t, \mathbf{U}) = 2\pi \sum_{n=0}^{\infty} h_{(n)_H} (2U_n - (M-1))q(t - nT), t \geq 0. \quad (3)$$

Here $(\cdot)_H$ denotes the modulo H operation and the modulation index for each symbol interval is chosen cyclically from the set $\{h_0, h_1, \dots, h_{H-1}\}$, $q(\cdot)$ is the phase shaping function. In order to ensure a finite number of states in the decoding trellis, modulation indices are restricted to the set of rational numbers with a common denominator P , such that $h_i = K_i/P$. The denominator P is always chosen such that $\text{gcd}(K_0, K_1, \dots, K_{H-1}, P) = 1$, where $\text{gcd}(\cdot)$ denotes the greatest common divisor of these arguments.

The excess phase in (3) can be written as

$$\phi(t, \mathbf{U}) = \pi \sum_{i=0}^{n-1} h_{(i)_H} (2U_i - (M-1)) + 2\pi \sum_{i=0}^{L-1} h_{(n-i)_H} (2U_{n-i} - (M-1))q(t - (n-i)T) \quad (4)$$

Substituting $\tau = t - nT$ such that the interval $t \in [nT, (n+1)T]$ is equivalent to $\tau \in [0, T]$, (4) becomes

$$\begin{aligned} \phi(\tau + nT, \mathbf{U}) &= 2\pi \sum_{i=0}^{n-1} h_{(i)_H} U_i + 4\pi \sum_{i=0}^{L-1} h_{(n-i)_H} U_{n-i} q(\tau + iT) \\ &\quad - 2\pi(M-1) \sum_{i=0}^{L-1} h_{(n-i)_H} U_{n-i} q(\tau + iT) - \pi(M-1) \sum_{i=0}^{n-L} h_{(i)_H} \end{aligned} \quad (5)$$

Second, we define the tilted phase for $t \in [nT, (n+1)T]$ as

$$\phi(t, \mathbf{U}) = \phi(t, \mathbf{U}) + \pi(M-1) \sum_{i=0}^{n-1} h_{(i)_H} + \frac{\pi(M-1)h_{(n)_H}(t - nT)}{T}. \quad (6)$$

Note that the sum of second and third term is actually the negative of the lowest trajectory of the excess phase trellis. When written in terms of τ , where $\tau \in [0, T]$, and substituting $\phi(\tau + nT, \mathbf{U})$ from (5), we get

$$\begin{aligned} \phi(\tau + nT, \mathbf{U}) &= 2\pi \sum_{i=0}^{n-1} h_{(i)_H} U_i + 4\pi \sum_{i=0}^{L-1} h_{(n-i)_H} U_{n-i} q(\tau + iT) \\ &\quad - 2\pi(M-1) \sum_{i=0}^{L-1} h_{(n-i)_H} q(\tau + iT) + \pi(M-1) \sum_{i=1}^{L-1} h_{(n-i)_H} + \frac{\pi(M-1)h_{(n)_H}\tau}{T} \end{aligned} \quad (7)$$

All the terms in $\varphi(\tau + nT, \mathbf{U})$ are periodic in n and depend only on the time translated variable τ . So the tilted phase transformation turns out to be a periodic function of time with period H .

On the time interval, $t \in [nT, (n+1)T]$, (7) can be expressed as

$$\varphi(t, \mathbf{U}) = 2\pi \sum_{i=0}^{n-L} h_{(i)_H} U_i + R(t-nT) + 4\pi \sum_{i=0}^{L-1} h_{(n-i)_H} U_{n-i} q(t-(n-i)T) \quad (8)$$

where $R(t)$ is a data independent term, and is defined as

$$R(t) = \pi(M-1) \sum_{i=1}^{L-1} h_{(n-i)_H} + \frac{\pi(M-1)h_{(n)_H}t}{T} - 2\pi(M-1) \sum_{i=0}^{L-1} h_{(n-i)_H} q(\tau+iT) \quad (9)$$

The tilted phase is generated from the input symbols by the CPE of (8). The CPE is a Finite State Machine (FSM) with a periodic coefficient $K_{(n)_H}$. Based on the relationship between the excess and tilted phase in (6), the CPE in (8), and the phase modulator in (2), we represent the multi-h CPM modulator as a periodic CPE followed by a memoryless modulator, as shown in Fig. 2. Here $Q_i(t, n) = 4\pi/P \cdot q(t-(n-i)T)$, the block labeled "TT" is the transformation in (6), and the double circled symbol denotes a modulo- P adder.

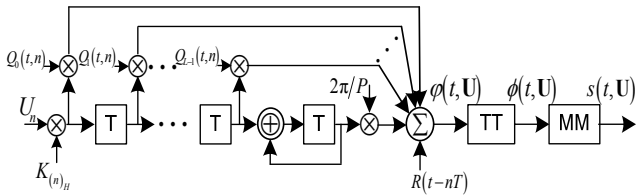


Fig. 2. Decomposition of multi-h CPM.

Unlike single-h CPM, where the state vector is defined as the cascade of the cumulative and the $L-1$ previous input symbols, for multi-h CPM we must also take the periodicity of the state machine into account. We define the state vector as

$$\boldsymbol{\chi}_n^{(y)} = \{\gamma_{n-L}, \mathbf{U}_{n-L+1}^{n-1}, (n)_H\} \quad (10)$$

where $\mathbf{U}_{n-L+1}^{n-1} = \{U_{n-L+1}, U_{n-L+2}, \dots, U_{n-1}\}$ is the set of past symbols determining the correlative terms in the tilted phase, $\gamma_n = \theta_n P/2\pi$, θ_n is called the cumulative phase state. Note that $(n)_H$ is incorporated in the state vector to conform to the usual definition of a state machine, i.e., the next state and output of the CPE is determined solely by the knowledge of the previous state and current input symbol.

3. Super Trellis Structure of Merged Encoder

Because of the existence of periodicity in the state machine, the trellis structure of CPE decomposed by multi-h CPM becomes complex, and much more difficult to draw with several indices. For simplicity, the super trellis structure with single-h CPM is presented and the minimum error event based on super trellis is analyzed firstly, then the analysis will be extended to the design of multiple trellis coded multi-h CPM system.

3.1 Construction of Super Trellis

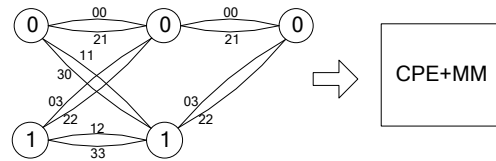


Fig. 3. Block diagram of multiple trellis coded CPM system.

The block diagram of multiple trellis coded CPM system is shown in Fig. 3. The multiple trellis encoder is a two-state conventional rate 1/2 encoder with multiple factor $k=2$. Parameters of the single-h CPM signaling are defined as: $M=4$, $h=1/4$, 1REC pulse shape. Such CPFSK (Continuous Phase Frequency Shift Keying) signaling with rectangular pulse shaping function with length $L=1$ is a simple form of full-response CPM.

The super trellis is defined as $S_1 S_2$, where S_1 and S_2 represent the trellis state of the multiple trellis encoder and the CPE respectively. As shown in Fig. 3, the trellis state of multiple trellis encoder is defined as 0 and 1, and the trellis state of the CPE is defined as $0, \pi/2, \pi$ and $3\pi/2$.

The super trellis structure of the merged encoder constructed by multiple trellis encoder and CPE is shown in Fig. 4. Based on the definition above, the state number of the merged encoder is the product of the state number of the multiple trellis encoder and CPE, e.g., the number of S_1 and S_2 is 2 and 4 respectively, so the state number of the merged encoder is $2 \times 4 = 8$.

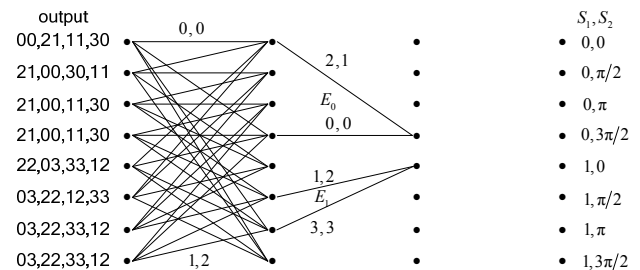


Fig. 4. Super trellis structure of merged encoder.

3.2 Error Event of Multiple Trellis Coded CPM

Based on analysis of super trellis structure as shown in Fig. 4, the occurrence of an error event of the merged encoder indicates the occurrence of the error event of the multiple trellis encoder and CPE simultaneously, and all the error events of the merged encoder must contain one or more error events of the multiple trellis encoder and CPE simultaneously. For example, an error event defining as E_0 occurred when trellis paths diverge at the same super state $S_1S_2 = 0,0$ and converge at the same super state $S_1S_2 = 0,3\pi/2$ after two transitions. The corresponding output of these two transitions is 0021 and 2100 respectively. The pairwise error sequence is defined as ξ , which is 0021-2100 for error event E_0 .

As shown in Fig. 4, there aren't parallel branches in the super trellis structure. So the minimum number of transitions of all error events is two at least, i.e., the error event with two transitions is the minimal error event, such as E_0 and E_1 . Also the number of symbols of the minimal error event is the effective length of the encoder, obviously, it is the product of the effective length of the multiple trellis encoder and CPE, e.g., the effective length of the multiple trellis encoder and CPE in Fig. 4 are both 2, so the effective length of the merged encoder is $2 \times 2 = 4$.

For single-h CPFSK, the effective length of the CPE is always 2, and no matter what kind of pairwise error sequence $A_1 \dots A_j - B_1 \dots B_j$ of the multiple trellis encoder is, the pairwise sequence $A_1 \dots A_j B_1 \dots B_j - B_1 \dots B_j A_1 \dots A_j$ must be the error sequence of the merged encoder. We define the error event with such error sequence as the "back-loop" error event, which is important in the analysis of the merged encoder with multi-h CPM, and the "back-loop" error event with $j = k$ (k is the multiple factor) must be the minimal error event in the merged encoder.

4. Design Procedure

The design procedure in this section could be divided into the following four steps.

4.1 Maximizing the Effective Length

For multiple trellis encoder, the effective length is the multiple factor k . Error events with cross transitions must have more symbols than error events with parallel transitions.

Based on the analysis of the super trellis structure, the effective length of the merged encoder is the product of the effective length of multiple trellis encoder and CPE. So maximizing the effective length of the merged encoder can be divided into maximizing the effective length of multiple trellis encoder and CPE each. The effective length of CPE is always 2 for single-h CPM because of the modulo P

(P is the denominator of the modulation index) adder operation. So the effective length of the merged encoder equals to $2k$ with single-h CPM.

For multi-h CPM, the effective length of the CPE can be always increased by proper use of several indices. However, the use of greater number of indices can not always guarantee the increase of the effective length of the CPE. For example, the "back-loop" error event E_0 with single-h CPFSK "0021-2100", at the same time, is the minimal error event of the merged encoder with dual-h CPFSK in cyclic use, i.e., the cyclic use of two indices fails to increase the effective length of the merged encoder when compared with single index. Therefore, compared with the number of indices, the proper use of them (pattern of indices) are more important in the design of maximizing the effective length of the merged encoder with multi-h CPM.

4.2 Maximizing Minimum Euclidean Distance

We first define $D^2(\xi)$ as the squared Euclidean distance with pairwise error sequence ξ , and D_{\min} as the minimum Euclidean distance among all these pairwise error sequences. For a superior code, D_{\min} is always generated by the minimal error event with effective length. In other words, if D_{\min} is generated by the error event in which the number of symbols is greater than the effective length, such code design is sure to be inferior. So the maximization of effective length and Euclidean distance is always jointly considered.

For multi-h CPM, the maximization of D_{\min} can be divided into the following three steps:

(1) The effective length of the merged encoder with single-h CPM is firstly analyzed, which equals to $2k$;

(2) For single-h CPM, the minimum Euclidean distance D_{\min} with the effective length $2k$ is maximized through a computer search to find the largest Euclidean distance among the pairwise error sequences like $0_1 0_2 \dots 0_k B_1 B_2 \dots B_k - B_1 B_2 \dots B_k 0_1 0_2 \dots 0_k$ with arbitrary values of $B_1 B_2 \dots B_k$, then the superior multiple trellis code based on such D_{\min} is designed, which is described in the following subsection 4.3;

(3) For multi-h CPM, the effective length is further maximized through designing the pattern of several indices, and the minimum Euclidean distance D_{\min} for multi-h CPM is further maximized based on the increase of effective length, which is described as following in subsection 4.4;

Since there is not any exact formula that describes $D^2(\xi)$ against h even for a given CPM signaling format, the maximization of D_{\min} is extremely difficult especially with several indices. For simplicity, the analysis is firstly based on the single-h CPM and then extended to multi-h CPM, firstly based on the effective length, and then extended to the minimum Euclidean distance, just as these three steps described above.

4.3 Multiple Trellis Code Design Following Ungerboeck's Set Partition Rules

Similarly to Ungerboeck's TCM design [16], the following two design rules are adopted.

- (1) All the diverging transition outputs from each state must be unique.
- (2) All the merging transition outputs to each state must be unique.

As an example, the multiple trellis code with dual-h CPM is designed, and parameters are listed as following: the code rate is 1/2, the state number of the multiple trellis code is 4, the multiple factor $k = 3$, the modulation alphabet $M = 4$, the modulation indices $[h_0, h_1] = [3, 4]/16$, and the memory length $L = 1$.

As analyzed in the previous subsection, multiple trellis code with single index $h = 1/4$ is firstly designed. The effective length of the multiple trellis encoder and CPE is 3 and 2 respectively, so the effective length of the merged encoder is 6. Then the minimum Euclidean distance is maximized through computer search among all the pairwise error sequences $000B_1B_2B_3 - B_1B_2B_3000$ with arbitrary $B_1B_2B_3$.

The largest Euclidean distance under search is 4, and the corresponding pairwise error sequence is 000202-202000. Following Ungerboeck's set partition rules, the multiple trellis code designed for single index CPFSK with $h = 1/4$ is shown in Fig. 5.

In most cases, the largest Euclidean distance under search cannot be accomplished in the code design. When the pairwise error sequence achieves the largest Euclidean distance, the Ungerboeck's set partition rules cannot always be obeyed at the same time, and other requirements are also need to satisfy which will be described later. In this case, the second or third largest Euclidean distance will be the alternative in the code design.

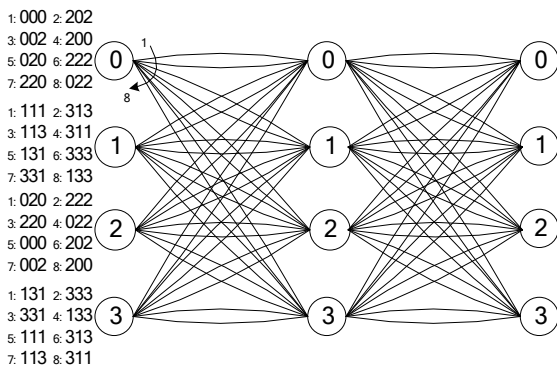


Fig. 5. Superior design for single index with $h = 1/4$.

After the design above, further verifying is need to make sure that the minimum Euclidean distance generated by the pairwise error sequence 000202-202000 is actually

the minimum one among all these pairwise error sequences. As shown in Fig. 5, the effective length of error events with parallel transitions and cross transitions is 3 and 6 respectively. Generally speaking, the Euclidean distance of error events with effective length 6 is larger than error events with effective length 3. However, the operation of verifying can not be neglected. In this case, the Euclidean distance with pairwise error sequence 000000020020-020020000000 and 000000002111-002111000000 is 6.22 and 4.68 respectively, which are both larger than 4 (parallel transitions), and the latter is proved to be the minimum one among all error events with cross transitions.

In the design of multiple trellis code, such pairwise error sequences as $A_1A_2A_3$ and $B_1B_2B_3$ with $(A_1 + A_2 + A_3) \bmod P = (B_1 + B_2 + B_3) \bmod P$ should be avoided, because such error sequences will result in the occurrence of the error event of multiple trellis encoder and CPE simultaneously. In this case, the effective length of the merged encoder will be shortened as to be 3. Similar case like $A_1 \dots A_j$ and $B_1 \dots B_j$ ($j < 2k$) with $(A_1 + \dots + A_j) \bmod P = (B_1 + \dots + B_j) \bmod P$ should also be avoided.

The error sequence with $h = 1/4$ which generates the largest Euclidean distance is also the same error sequence with $[h_0, h_1] = [3, 4]/16$ which also generates the largest Euclidean distance, i.e., the superior design of multiple trellis code for single index with $h = 1/4$ is always the superior one for two indices with $[h_0, h_1] = [3, 4]/16$. It can be proved because $h \approx \text{average}[h_0, h_1]$.

One may doubt that the code design in Fig. 5 is not superior for single-h with $h = 1/4$ (i.e. $P = 4$), because the pairwise error sequence 000-202 satisfies $(0 + 0 + 0) \bmod 4 = (2 + 0 + 2) \bmod 4$. In fact it really isn't and that doubt is reasonable.

However, the code design in Fig. 5 is actually the superior one for dual-h with $[h_0, h_1] = [3, 4]/16$ because $((-3) \cdot 3 + (-3) \cdot 4 + (-3) \cdot 3) \bmod 16 \neq (1 \cdot 3 + (-3) \cdot 4 + 1 \cdot 3) \bmod 16$, and it could be verified later.

4.4 Design of Pattern of Several Indices

Based on the superior design of multiple trellis code with single-h CPM in the previous subsection, the effective length with multi-h CPM can be further maximized by a proper pattern design of these several indices.

Before the analysis, the state transfer diagram of the superior multiple trellis code designed above is shown in Fig. 6. As shown in the diagram, the exponent of J and D represents the number of transitions and the symbol weight respectively between two states. For example, $J(D^2 + D^2)$ represents that there are one transition and two parallel branches from the state "A" to state "B", and the symbol weight of two branches are both 2. Note that the definition on the exponent of D is different with the

traditional analysis on the convolutional code, which is hamming distance always.

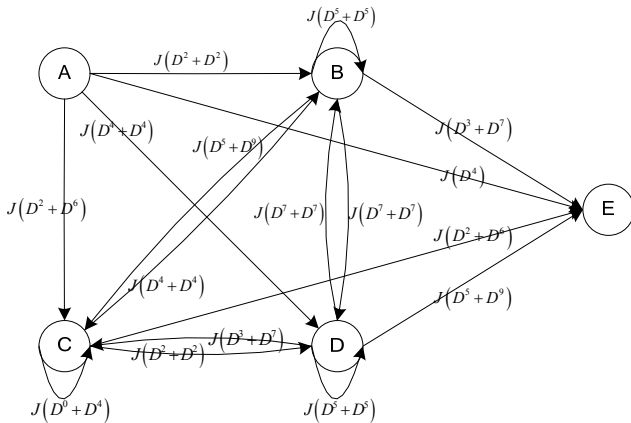


Fig. 6. State transfer diagram of the designed multiple trellis encoder.

Based on the state transfer diagram, the state transfer equations are listed as follows:

$$\begin{cases} X_B = J(D^2 + D^2)X_A + J(D^5 + D^5)X_C + J(D^4 + D^4)X_D + J(D^7 + D^7)X_E \\ X_C = J(D^2 + D^6)X_A + J(D^5 + D^9)X_B + J(D^0 + D^4)X_D + J(D^3 + D^3)X_E \\ X_D = J(D^4 + D^4)X_A + J(D^7 + D^7)X_B + J(D^2 + D^2)X_C + J(D^5 + D^5)X_E \\ X_E = J(D^4)X_A + J(D^3 + D^3)X_B + J(D^2 + D^6)X_C + J(D^5 + D^9)X_D \end{cases} \quad (11)$$

Solving these equations, we get the state transfer function as:

$$T(D, J) = \frac{JD^4 + 2J^2D^5 + J^2D^8 + J^2D^{12} + 2J^2D^{13} - 2J^3D^5 - 4J^3D^{10} + J^3D^{13} + 4J^3D^{14}}{1 - J - JD^4 - 4JD^5 + 2J^2D^5 + 4J^2D^{10} - 2J^2D^{13} - 4J^2D^{14}} \quad (12)$$

Obviously, JD^4 is the minimum polynomial in $T(D, J)$, and it also represents the minimal error event of the multiple trellis encoder, so the analysis on error events before is verified by the state transfer function, and the further maximization of effective length with several indices is just based on this state transfer function.

We define \mathcal{E} as symbol difference between the two corresponding symbols and $D(\mathcal{E})$ as the sum of symbol differences in the pairwise error sequence.

For single-h CPM, the design criteria is to maximize the minimal transitions which satisfies

$$D(\mathcal{E}) \bmod P = 0 \quad (13)$$

where P is the denominator of the modulation index, which is 4 with $h = 1/4$. The “back-loop” error event defined above with the pairwise error sequence 000202-202000 must satisfy (13), because $D(\mathcal{E})$ of such error event must be zero, which satisfies equation (13) obviously no matter P is. Note that the pairwise error sequence 000-202 also satisfies (13) because $D(\mathcal{E}) = 4$. So the minimal transitions we could maximize is 1 actually, and the effective length of the merged encoder is shortened to be $k = 3$.

For multi-h CPM with $[h_0, h_1, \dots, h_{H-1}] = [K_0, K_1, \dots, K_{H-1}]/P$, the design criteria is also to maximize the minimal transitions which satisfies

$$\begin{cases} K_0\varepsilon_0 + K_1\varepsilon_1 + \dots + K_{|\xi|-1}\varepsilon_{|\xi|-1} \bmod P = 0 \\ \varepsilon_0 + \varepsilon_1 + \dots + \varepsilon_{|\xi|-1} = D(\mathcal{E}) \end{cases} \quad (14)$$

Here $D(\mathcal{E})$ is the exponent of polynomials with dummy variable “ D ” in equation (12), or the addition (subtraction) of the exponent of several polynomials, which is corresponding to the concatenated error events in the pairwise error sequence. The subscript $|\xi|$ is the length of the pairwise error sequence ξ .

For example, we analyze the case of dual-h CPM with $[h_0, h_1] = [3, 4]/16$ in cyclic use. “Back-loop” error events of several polynomials in (12) have been checked with criteria in (14). Results are shown in Tab. 1.

Polynomial	Pairwise error sequence	Whether satisfies (14)
JD^4	000202-202000	No
J^2D^4	000000020020-020020000000	Yes
J^2D^{12}	000000222222-222222000000	Yes
...

Tab. 1. Validation results.

From Tab. 1, pairwise error sequence 000000020020-020020000000 has been verified firstly to satisfy (14), so the minimal transitions we could maximize is 4, hence the effective length of the merged encoder with two indices $[h_0, h_1] = [3, 4]/16$ in cyclic use is $4k = 12$. The effective length could be further increased by a proper pattern design of the two indices. The pattern includes the number and the periodicity of these indices. Generally speaking, it is much more complex to deal with a great number of modulation indices, and it is relatively manageable to just increase the periodicity with some few indices.

For the case of two indices with $[h_0, h_1] = [3, 4]/16$, the periodicity could be increased to $Q (Q \geq 3)$ by use of the pattern like $[h_{0,0}, \dots, h_{0,i-1}, h_{1,0}, \dots, h_{1,j-1}]$, ($i+j = Q$), which means that the number of h_0 and h_1 is i and j respectively. Obviously, the larger Q is, the larger effective length we could maximize for the merged encoder.

As we know, the minimal error event with JD^4 and the minimal “back-loop” error event with J^2D^0 are the “bottle-neck” in the maximization of the periodicity Q . Details of the maximization process are shown in Tab. 2. The last column indicates whether satisfying (14) with the “bottle-neck” error event or not.

The largest Q we could maximize is 10 from Tab. 2, because patterns with $Q (Q > 10)$ all satisfy (14) for the minimal “back-loop” error event. Also for arbitrary number of indices H , the maximal Q we could get is $Q_{\max} = 5H$, because once $Q > 5H$, there must be one pattern with at

least 6 same consecutive indices, which means single index for the minimal “back-loop” error event, and then the effective length will be shorten greatly. Once the maximal Q has been achieved, the next step is to compute the effective length of the merged encoder for dual-h CPM with a pattern like $[h_0, h_0, h_0, h_0, h_0, h_1, h_1, h_1, h_1, h_1]$.

Q	Pattern	Whether satisfies (14)
3	$[h_0, h_0, h_1]$	No
4	$[h_0, h_0, h_0, h_1]$	No
5	$[h_0, h_0, h_0, h_1, h_1]$	No
	$[h_0, h_0, h_0, h_0, h_1]$	No
6	$[h_0, h_0, h_0, h_0, h_1, h_1]$	No
	$[h_0, h_0, h_0, h_0, h_0, h_1]$	No
7	$[h_0, h_0, h_0, h_0, h_1, h_1, h_1]$	No
	$[h_0, h_0, h_0, h_0, h_0, h_1, h_1]$	No
	$[h_0, h_0, h_0, h_0, h_0, h_0, h_1]$	Yes
8	$[h_0, h_0, h_0, h_0, h_0, h_1, h_1, h_1]$	No
	$[h_0, h_0, h_0, h_0, h_0, h_0, h_1, h_1]$	Yes
	$[h_0, h_0, h_0, h_0, h_0, h_0, h_0, h_1]$	Yes
9	$[h_0, h_0, h_0, h_0, h_0, h_1, h_1, h_1, h_1]$	No
	$[h_0, h_0, h_0, h_0, h_0, h_0, h_1, h_1, h_1]$	Yes
	$[h_0, h_0, h_0, h_0, h_0, h_0, h_0, h_1, h_1]$	Yes
	$[h_0, h_0, h_0, h_0, h_0, h_0, h_0, h_0, h_1]$	Yes
10	$[h_0, h_0, h_0, h_0, h_0, h_1, h_1, h_1, h_1, h_1]$	No
	$[h_0, h_0, h_0, h_0, h_0, h_0, h_1, h_1, h_1, h_1]$	Yes
	$[h_0, h_0, h_0, h_0, h_0, h_0, h_0, h_1, h_1, h_1]$	Yes
	$[h_0, h_0, h_0, h_0, h_0, h_0, h_0, h_0, h_1, h_1]$	Yes
...	...	Yes

Tab. 2. Details of the maximization of Q .

Polynomials in (12) have been verified one by one. Because the greatest common divisor of the multiple factor $k=3$ and the periodicity $Q=10$ is 1, i.e., $\gcd(k, Q)=1$. So the minimal error event of the multiple trellis encoder for dual-h CPM with such pattern is ten repeated error events corresponding to JD^4 , i.e., $000\cdots000-202\cdots202$, and the value of $(K_0\varepsilon_0 + \dots + K_{29}\varepsilon_{29} = 140) \bmod 16 \neq 0$. Hence, the “back-loop” error event of this pattern $000\cdots000202\cdots202-202\cdots202000\cdots000$ is the minimal error event of the merged encoder because $(K_0\varepsilon_0 + \dots + K_{59}\varepsilon_{59} = 140) \bmod 16 = 0$, so the effective length of the merged encoder is 60, and the minimum Euclidean distance can be further maximized based on such effective length. The larger the number of the modulation indices is, the larger the periodicity Q could be achieved, and the larger the effective length of the merged encoder could be maximized. Based on the maximization of effective length and the minimum Euclidean distance, further

verifying is necessary to guarantee the performance optimization.

Based on the analysis above, further verifying is necessary. Polynomials in (12) and “back-loop” error events of them with J^T ($T < 2Q$) must be verified one by one with pattern as $[h_0, h_0, h_0, h_0, h_0, h_1, h_1, h_1, h_1, h_1]$. Once one of them has been verified to satisfy (14), the number of minimal transitions will be shortened, and also the effective length and the Euclidean distance will be reduced. Obviously, the process of verifying is very complex and time-consuming. However, it can not be neglected, and it can be done by computer search, and it makes the design effective and rigorous.

The procedure of multiple trellis code design with multi-h CPM is presented in this section. With the increase of multiple factor k and the state number of super trellis, the design becomes much more complex even with the aid of computer searching and verifying. However, several presented rules have been proved valuable, and make the design procedure much more effective.

5. Performance Analysis

Based on the analysis above, the minimal error events are those pairwise error sequences with the effective length 60 for dual-h CPM with $[h_0, h_1] = [3, 4]/16$ by use of pattern like $[h_0, h_0, h_0, h_0, h_0, h_1, h_1, h_1, h_1, h_1]$. Because of the huge complexity of (12), the state transfer function is rewritten just related with J and J^2 as following:

$$T(D, J) = \frac{JD^4 + 2J^2D^5 + J^2D^8 + J^2D^{12} + 2J^2D^{13} - 2J^2D^5 - 4J^3D^{10} + J^3D^{13} + 4J^3D^{14}}{1 - J - JD^4 - 4JD^5 + 2J^2D^5 + 4J^2D^{10} - 2J^2D^{13} - 4J^2D^{14}} = JD^4 + J^2D^4 + 2J^2D^5 + 2J^2D^8 + 4J^2D^9 + J^2D^{12} + 2J^2D^{13} + \dots \quad (15)$$

From (15), polynomials with J^2D^0 (“back-loop” error event of JD^4), J^2D^4 , $2J^2D^5$, $2J^2D^8$, $4J^2D^9$, J^2D^{12} and $2J^2D^{13}$ are corresponding to these minimal error events generating the minimum Euclidean distance, and polynomials with J^T ($T \geq 3$) have been verified to generate longer effective length and larger Euclidean distance.

In [17] it is shown that the bit error probability of coded continuous phase modulation is upper bounded by

$$P_b \leq \sum_d C_d Q\left(\sqrt{d^2 E_b/N_0}\right) = C_{d_{\min}} Q\left(\sqrt{d_{\min}^2 E_b/N_0}\right) + \text{other terms} \quad (16)$$

where the summation is over all Euclidean distances in the set of all error events, d_{\min}^2 is the smallest of these distances and is referred to as the normalized squared free Euclidean distance which equals to $D_{\min}^2/2E_b$. $Q(x)$ is defined as

$$Q(x) = \frac{1}{\sqrt{2\pi}} \int_x^\infty e^{-y^2/2} dy. \quad (17)$$

According to the state transfer function $T(D, J)$,

d_{\min}^2 and $C_{d_{\min}}$ of several terms in (15) corresponding to the minimal error events are listed in Tab. 3.

No. i	Polynomial	Pairwise error sequence	$d_{\min}^2(i)$	$C_{d_{\min}}^i$
1	J^2D^0	000202-202000	31.62	40
2	J^2D^4	000000-020020	29.78	20
3,4	$2J^2D^5$	000000-002111 000000-200111	25.50 32.78	40
5,6	$2J^2D^8$	000000-020222 000000-222020	29.78 29.46	40
7~10	$4J^2D^9$	000000-002313 000000-200313 000000-220131 000000-022131	24.00 31.27 26.42 26.25	60
11	J^2D^{12}	000000-222222	29.78	60
12,13	$2J^2D^{13}$	000000-220333 000000-022333	28.01 27.84	80

Tab. 3. d_{\min}^2 and $C_{d_{\min}}$ of several polynomials

These thirteen polynomials in Tab. 3 almost determine the error bit probability in (16), and we get the truncated bound as

$$P_b \leq \sum_d C_d Q\left(\sqrt{d^2 E_b/N_0}\right) \approx \sum_{i=1}^{13} C_{d_{\min}}^i Q\left(\sqrt{d_{\min}^2(i) E_b/N_0}\right). \quad (18)$$

As seen in the table, the value of $C_{d_{\min}}^i$ is very large, and it should not be ignored in the computation of bit error probability in (18).

6. Numerical Results and Discussion

6.1 Rate 1/2 Encoded $[h_0, h_1] = [3, 4]/16$ Quaternary CPFSK ($R = 1$ bit/symbol)

We define R as the number of bits in information per modulation symbol. Numerical results for $R = 1$ bit/symbol are shown in Fig. 7, the dashed line indicates the performance of uncoded MSK, and the three solid lines indicate the truncated bounds of the three rate 1/2 coded quaternary CPFSK schemes, also simulation results of the three schemes are given for comparison. The first one is the conventional convolutional code with generation polynomial (7, 5) in octal form, which is combined with single-h CPFSK with $h = 1/4$; the second one is the multiple trellis code with multiple factor $k = 2$ as shown in Fig. 3, which is combined with dual-h CPFSK with $[h_0, h_1] = [3, 4]/16$; the third one is the multiple trellis coded with multiple factor $k = 3$ as shown in Fig. 5, which is also combined with dual-h CPFSK with $[h_0, h_1] = [3, 4]/16$.

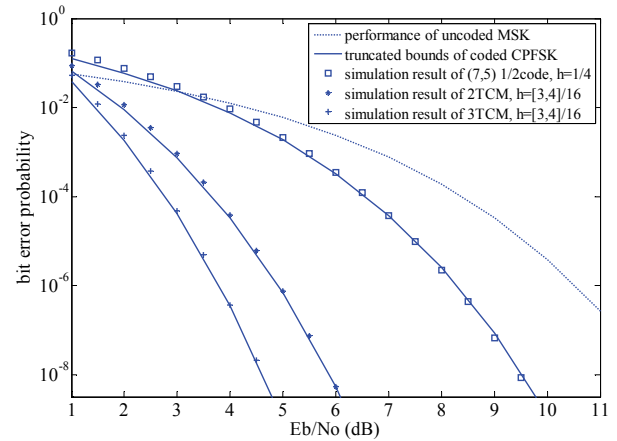


Fig. 7. Numerical results with four $R = 1$ bit/symbol schemes.

As shown in Fig. 7, simulation results are consistent with the truncated bounds for the three schemes. In Conclusion, performance of coded CPFSK schemes are generally better than the uncoded MSK, the multiple trellis codes combined with dual-h CPFSK are much better than the convolutional code combined with single-h CPFSK, and with the increase of multiple factor, further performance gain can be achieved. Compared with uncoded MSK, the convolutional code, multiple trellis code with $k = 2$ and $k = 3$ can achieve 2.2 dB, 5.6 dB and 6.8 dB coding gains respectively when bit error probability is 10^{-6} .

For brevity, multiple trellis code with larger multiple factor has not been simulated. In Tab. 4, d_{\min}^2 and $C_{d_{\min}}$ of the best rate 1/2 multiple trellis code design with $[h_0, h_1] = [3, 4]/16$ are given. The comparison assumes that the trellis encoders are of the same rate, measured in bits of information per modulation symbol as in previous work. Since rate 1/2 coded $[h_0, h_1] = [3, 4]/16$ quaternary CPFSK has approximately the same spectral efficiency as MSK, performance is compared to MSK. Coding gain is defined as $10 \cdot \log_{10}(d_{\min}^2/d_{\text{MSK}}^2)$, where $d_{\text{MSK}}^2 = 2$ is the minimum squared Euclidean distance of MSK. It can be seen that the new coding scheme yields superior d_{\min}^2 and the increase in performance gain for k equals to 5 is almost 7.5 dB.

k	d_{\min}^2	$C_{d_{\min}}$	Gain(dB) over MSK
2	17.54	44	5.6
3	24.00	60	6.8
4	28.82	72	7.2
5	31.46	88	7.5

Tab. 4. Results for rate 1/2 modulo-4 encoded $[h_0, h_1] = [3, 4]/16$ quaternary CPFSK.

6.2 Rate 2/3 Encoded $[h_0, h_1] = [3, 4]/32$ Octal CPFSK ($R = 2$ bits/symbol)

In Fig. 8, numerical results for $R = 2$ bits/symbol are given, the dashed line indicates the performance of

uncoded quaternary CPFSK with $h = 1/4$, and the two solid lines indicate the truncated bounds of the two rate 2/3 coded octal CPFSK schemes, also the two schemes are simulated for comparison. The first one is the superior convolutional code with generation polynomial (17, 06, 15) in octal form, which is combined with single-h CPFSK with $h = 1/8$; the second one is the multiple trellis code with multiple factor $k = 2$ as shown in Fig. 9, which is combined with dual-h CPFSK with $[h_0, h_1] = [3, 4]/32$. When bit error probability is 10^{-6} , the convolutional code with single-h and the multiple trellis code with dual-h are 1.9dB and 4.3dB better than the uncoded quaternary CPFSK schemes respectively.

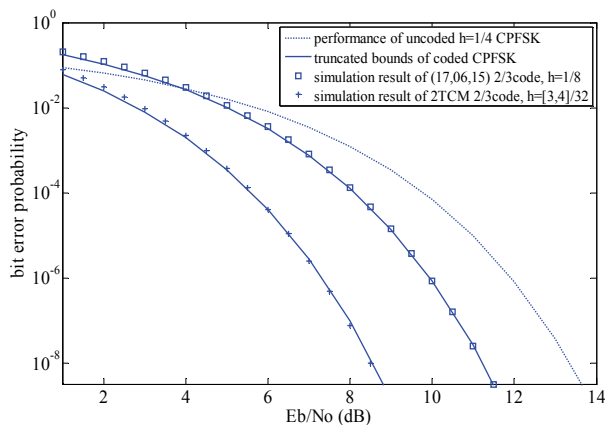


Fig. 8. Numerical results with three $R = 2$ bits/symbol schemes.

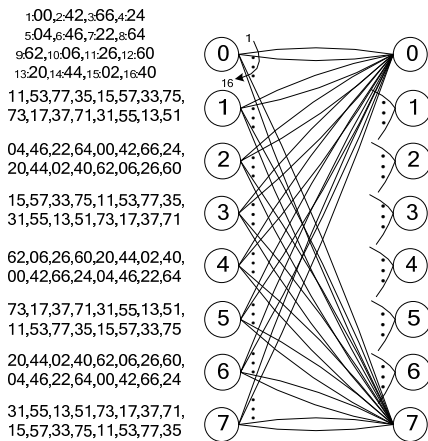


Fig. 9. Superior rate 2/3 code design for dual-h with $[h_0, h_1] = [3, 4]/32$.

In Tab. 5, d_{\min}^2 and $C_{d_{\min}}$ of the best rate 2/3 code design with $[h_0, h_1] = [3, 4]/32$ are given. Since rate 2/3 coded $[h_0, h_1] = [3, 4]/32$ octal CPFSK has approximately the same spectral efficiency as $h = 1/4$ quaternary CPFSK ($d_{\min}^2 = 1.45$), coding gain is compared to that modulator. It can be concluded that the new coding scheme yields performance superior to the uncoded quaternary CPFSK. The reported code searches are not complete in this table because of the large complexity.

k	d_{\min}^2	$C_{d_{\min}}$	Gain(dB) over $h = 1/4$ quaternary CPFSK
2	10.38	40	4.7
3	16.56	48	5.6
4	20.85	60	6.1
5	23.42	72	6.5

Tab. 5. Results for rate 2/3 modulo-8 encoded $[h_0, h_1] = [3, 4]/32$ octal CPFSK.

Great performance gain could be achieved by adopting two indices in multiple trellis coded CPM system as shown in Tab. 4 and 5. The expense of such performance gain is the large number of super states and the large decision depth, i.e., corresponding to the great increase of the system complexity. The reason is that joint demodulation and decoding is accomplished based on super trellis structure by Viterbi algorithm at the receiver side and the decision depth is large enough (up to hundreds of symbols, usually 5 to 7 times of the effective length) to guarantee the performance. The large decision depth brings out long data delay and huge memory and processing units, which means great complexity for the receiver. Besides, superbaud timing is also necessary for the recovery of the multi-h pattern at the receiver side, and the larger the periodicity Q is, the much more complex the recovery of superbaud timing will become.

7. Conclusion

This paper has presented the design of the superior multiple trellis encoder combined with multi-h CPM based on the super trellis structure of the merged encoder and the pattern design of several indices. System performance has been analyzed based on the state transfer function of the encoder. Comparison results show that this new coding scheme consistently obtains better performance than previous schemes. With the increase of multiple factor, more performance gains could be achieved at the expense of larger complexity.

References

- [1] Department of Defense Interface Standard. Interoperability standard for single-access 5-kHz and 25-kHz UHF satellite communications channels. *MIL-STD188-181B*, Mar. 1999.
- [2] GEOGHEGAN, M. Description and performance results for a multi-h CPM telemetry waveform. In *Proc. 21st Century MILCOM Conf.*, vol. 1, 2000, p. 353-357.
- [3] WILSON, S., HIGHFILL, J., HSU, C.-D. Error bounds for multi-h phase codes. *IEEE Trans. Commun.*, Jul. 1982, vol. 28, p. 660 to 665.
- [4] XIONG, E, BHATMULEY, S. Performance of MHPM in Rician and Rayleigh flat fading mobile channels. *IEEE Trans. Commun.*, Mar. 1997, vol. 45, p. 279 - 283.

- [5] DAVE, B. A., RAO, K. R. Generalized asymmetric multi-h phase coded modulation for M-ary data transmission. In *Canadian Conference on Electrical and Computer Engineering (IEEE CCECE)*. Niagara Falls, May 2004, p. 559 - 562.
- [6] SASASE, I., MORI, S. Multi-h phase-coded modulation. *IEEE Commun. Mag.*, 1991, p. 46 - 56.
- [7] FONSEKA, J. P., DAVIS, G. R. Combined coded multi-h CPFSK signalling. *IEEE Trans. Commun.*, Oct. 1990, vol. 38, p. 1708 to 1715.
- [8] ERTAS, T., POON, F. S. F. Trellis coded multi-h CPM for power and bandwidth efficiency. *Electron. Lett.*, 1993, vol. 29, no. 2, p. 229 - 230.
- [9] KIM, H., STÜBER, G. L. Turbo-like coded multi-h continuous phase modulation. *IEEE Military Communications Conference*, 2004, p. 352 - 358.
- [10] NARAYANAN, K. R., STÜBER, G. L. Performance of trellis-coded CPM with iterative demodulation and decoding. *IEEE Trans. Commun.*, Apr. 2001, vol. 49, p. 676 - 687.
- [11] MOQVIST, P., AULIN, T. M. Serially concatenated continuous phase modulation with iterative decoding. *IEEE Trans. Commun.*, Nov. 2001, vol. 49, no. 11, p. 1901 - 1915.
- [12] FONSEKA, J. P. Nonlinear continuous phase frequency shift keying. *IEEE Trans. Commun.*, 1991, vol. 39, no. 10, p. 1473 to 1481.
- [13] DIVSALAR, D., SIMON, M. K. Multiple trellis coded modulation (MTCM). *IEEE Trans. Commun.*, 1988, vol. 36, no. 4, p. 410 to 419.
- [14] RIMOLDI, B. E. A decomposition approach to CPM. *IEEE Trans. Inform. Theory*, 1988, vol. 34, no. 2, p. 260 - 270.
- [15] SALEEM, S., STÜBER, G. L. Trellis termination of multi-h CPM and the diophantine Frobenius problem. *IEEE Tran. Commun.*, August 2011, vol. 59, no. 8, p. 2196-2205.
- [16] UNGERBOECK, G. Channel coding with multilevel phase signals. *IEEE Trans. Inform. Theory*, Jan. 1982, vol. IT-28, p. 56 - 67.
- [17] LINDELL, G., SUNDBERG, C.-E. W. An upper bound on the bit error probability of combined convolutional coding and continuous phase modulation. *IEEE Trans. Inform. Theory*, Sep. 1988, vol. 34, no. 5, p. 1263 - 1269.

About Authors

LIU Xian was born in 1981. He received his Master degree from PLA University of Science and Technology in 2006. His research interests include modulation and coding theory.

LIU Aijun was born in 1970. He received his Doctor degree from PLA University of Science and Technology in 1999. His research interests include satellite communications.

ZHANG Bangning was born in 1963. He received his Doctor degree from PLA University of Science and Technology in 1992. His research interests include anti-jamming in satellite communications.

PAN Kegang was born in 1979. He received his Doctor degree from PLA University of Science and Technology in 2007. His research interests include synchronization theory.